energy&fuels

Article

pubs.acs.org/EF

Comparative Assessment of Gasification Based Coal Power Plants with Various CO_2 Capture Technologies Producing Electricity and Hydrogen

Sanjay Mukherjee,[†] Prashant Kumar,*[,†] Ali Hosseini,[‡] Aidong Yang,[§,∥] and Paul Fennell[⊥]

[†]Department of Civil and Environmental Engineering, Faculty of Engineering and Physical Sciences (FEPS), University of Surrey, Guildford, Surrey GU2 7XH, United Kingdom

[‡]Sharif Energy Research Institute (SERI), Sharif University of Technology, Tehran, Iran

[§]Department of Chemical and Process Engineering, FEPS, University of Surrey, Guildford, Surrey GU2 7XH, United Kingdom

[∥]Department of Engineering Science, University of Oxford, Parks Road, Oxford OX1 3PJ, United Kingdom

[⊥]Department of Chemical Engineering, Imperial College London, South Kensington, London SW7 2AZ, United Kingdom

Supporting Information

ABSTRACT: Seven different types of gasification-based coal conversion processes for producing mainly electricity and in some cases hydrogen (H_2), with and without carbon dioxide (CO_2) capture, were compared on a consistent basis through simulation studies. The flowsheet for each process was developed in a chemical process simulation tool "Aspen Plus". The pressure swing adsorption (PSA), physical absorption (Selexol), and chemical looping combustion (CLC) technologies were separately analyzed for processes with CO_2 capture. The performances of the above three capture technologies were compared with respect to energetic and exergetic efficiencies, and the level of CO_2 emission. The effect of air separation unit (ASU) and gas turbine (GT) integration on the power output of all the CO_2 capture cases is assessed. Sensitivity analysis was carried out for the CLC process (electricity-only case) to examine the effect of temperature and water-cooling of the air reactor on the overall efficiency of the process. The results show that, when only electricity production in considered, the case using CLC technology has an electrical efficiency 1.3% and 2.3% higher than the PSA and Selexol based cases, respectively. The CLC based process achieves an overall CO_2 capture efficiency of 99.9% in contrast to 89.9% for PSA and 93.5% for Selexol based processes. The overall efficiency of the CLC case for combined electricity and H_2 production is marginally higher (by 0.3%) than Selexol and lower (by 0.6%) than PSA cases. The integration between the ASU and GT units benefits all three technologies in terms of electrical efficiency. Furthermore, our results suggest that it is favorable to operate the air reactor of the CLC process at higher temperatures with excess air supply in order to achieve higher power efficiency.

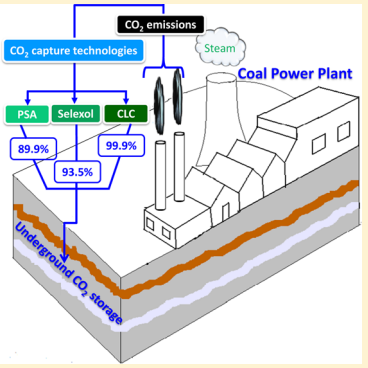

1. INTRODUCTION

Energy is the backbone of every modern society. On the other hand, its production is one of the key contributors toward the global climate change. In particular, power plants produce both electricity and CO_2 by combusting fossil fuels, which is one of the major sources of total man made CO_2 emissions worldwide.[1,2] Future forecasts for the economic growth in Asia Pacific and industrial development in Africa indicate that the total world energy demand will increase from 462 quadrillion British Thermal Units (BTU) in 2005 to over 695 quadrillion BTU by 2030.[3] The exponential rise in emissions of CO_2 from fossil fuel utilization to around 30 Gt per year will lead to significant climate change unless the emissions are captured and stored.[4]

Developing clean and affordable energy with abundant supply is an issue of international concern. Until recently, the prime focus of the research on power generation was on improving energy efficiency and switching from fossil fuels toward less carbon intensive (renewable) energy sources. The renewable energy technologies can reduce CO_2 emissions but are still costly. Even if they are made cost-competitive in the next few years, they will still need time to penetrate the market. Some researchers consider coal as the primary source of energy at least for the next 5−6 decades since its supply will last over 150 years compared with 50−60 years for oil and natural gas.[5] Thus, there is a large international research effort toward developing technologies to use coal in an environmentally sustainable manner.[6]

In the recent years, carbon capture and storage (CCS) has been considered to offer "end-of-pipe" technologies that can allow continuous use of fossil fuels with low or almost negligible emissions. A review by Boot-Handford et al.[7] has

Received: December 9, 2013
Revised: January 20, 2014
Published: January 21, 2014

Table 1. Summary of Literature Review on the Comparison of Different Coal to Electricity and H_2 Conversion Technologies with and without CCS

study	conversion technology used	fuel type	CO_2 capture technology used	electrical efficiency (% LHV)	H_2 efficiency (% LHV)	CO_2 capture efficiency (%)	overall efficiency (% LHV)
Wheeler[35]	IGCC	coal			50.9		50.9
			post-combustion/chemical absorption (amine)		43.4	97.4	43.4
Doctor et al.[36]	IGCC	coal	pre-combustion/physical absorption (Selexol)	12.8	44.5	86.8	57.3
Klett et al.[37]	IGCC	coal		4.5	51.0		55.5
			pre-combustion/physical absorption (Selexol)	1.4	51.9	92.0	53.3
Parsons[38]	subcritical PC	coal (bituminus)		38.9			396.8
			post-combustion/chemical absorption (MEA)	27.7		99.5	27.7
	NGCC	natural gas		57.9			57.9
			Post-Combustion/Chemical Absorption (MEA)	49.9		90	49.9
	IGCC (Shell)	coal (bituminus)		47.4			47.4
			post-combustion/chemical absorption (MEA)	40.1		90.2	40.1
Chiesa et al.[8]	IGCC with syngas quench	coal		42.6			42.6
			pre-combustion/physical absorption (Selexol)	36.8		91.3	36.8
				4.21	57.46		61.7
			pre-combustion/physical absorption (Selexol)	2.1	57.46	91.28	59.6
Damen et al.[9]	subcritical	coal (bituminus)	post-combustion/chemical absorption (MEA)	35.0		88	35.0
	IGCC		pre-combustion/physical absorption (Selexol)	43.0		85	43.0
			post-combustion/chemical absorption (MEA)	37.0−38.0		90	37.0−38.0
	NGCC	natural gas	post-combustion/chemical absorption (MEA)	47.0		85	47.0
Chiesa et al.[39]	NGCC	natural gas	CLC with SC	0.45	77.4	∼100	78.1
			CLC with CT	17.57	49.7	∼100	76.6
	NGCC (FTR-)		post-combustion/chemical absorption (MEA)	0	78.0	73.6	78.0
Li and Fan[13]	pressurized fluidized bed combustor	coal (Illinois #6)		38.0−45.0 (HHV)			38.0−45.0 (HHV)
			post-combustion/chemical absorption (MEA)	26.6−31.5 (HHV)		90	26.6-31.5 (HHV)
Rezvani et al.[40]	IGCC	coal (bituminous)		45.4			45.4
			pre-combustion/physical absorption (Selexol)	35.6		91	35.6
			pre-combustion/membrane separation	36.4		93	36.4
			CLC	35.2		∼100	35.2
Cormos[10]	IGCC with water quench	coal	pre-combustion/physical absorption (Selexol)	36.0		92.35	36.0
				28.6	12.9	92.35	41.5
		coal with municipal solid waste		35.8		92.83	35.8
		coal with meat and bone meal		35.7		93.0	35.7
		coal with sawdust		37.2		92.2	37.2
Fan and Li[43]	IGCC	coal (Illinois #6)	post-combustion/chemical absorption (MEA)	32.1 (HHV)		90	32.1 (HHV)
			CLC	36.5 (HHV)		100	36.5 (HHV)
	gasification based coal to H_2 process		post-combustion/chemical absorption (MEA)	2.1 (HHV)	55.7 (HHV)	90	57.8 (HHV)
	IGCC		CLC	26.0 (HHV)	38.1 (HHV)	100	64.1 (HHV)
Cormos[12]	IGCC (entrained flow gasifier)	coal		46.6			46.6
			pre-combustion/physical absorption (Selexol)	37.1		90.79	37.1
			CLC	38.38		99.55	38.38
Fan et al.[23]	PC	coal		36.8 (HHV)			36.8

dx.doi.org/10.1021/ef4024299 | Energy Fuels 2014, 28, 1028−1040

Table 1. continued

study	conversion technology used	fuel type	CO_2 capture technology used	electrical efficiency (% LHV)	H_2 efficiency (% LHV)	CO_2 capture efficiency (%)	overall efficiency (% LHV)
			post-combustion/chemical absorption (MEA)	26.2 (HHV)		90	26.2 (HHV)
	coal direct chemical looping (CDCL)		CLC	34.7 (HHV)		~100	34.7 (HHV)

comprehensively discussed the recent developments, challenges, and potential future improvements in different types of CCS technologies. Table 1 shows a summary of a number of studies on selection of a promising CCS technology that can produce electricity and, in some cases, H_2 from fossil fuels. For instance, Chiesa et al.[8] compared different scenarios considering CO_2 venting and CO_2 capture using integrated gasification combined cycle (IGCC) technology for the production of H_2 and electricity from coal. Physical absorption and adsorption processes were assumed for CO_2 and H_2 separation, respectively. They[8] concluded that, with an emissions constraint, there are very small thermodynamic benefits of coproduction relative to stand-alone electricity and H_2 production. Damen et al.[9] reviewed various concepts including oxyfuel combustion, membrane separation, physical absorption, and chemical absorption processes for electricity and H_2 production from coal and natural gas with CCS. A number of critical factors were identified and compared, including efficiency, cost of energy (COE), cost of H_2 (COH), and CO_2 avoidance costs. Also assessed were the impact of fuel prices on electricity and H_2 production costs for pulverized coal (PC), natural gas combined combustion (NGCC), and IGCC plants. The analysis showed that with CO_2 capture, the net electrical efficiencies are 30−35% for PC, 32−40% for IGCC, and 43−50% for NGCC power plants. Also, both the chemical and physical absorption processes can achieve 85−90% CO_2 capture efficiency with the precapture technologies being more suitable for IGCC plants. Cormos[10] describes the methodology to evaluate the performance of a coproduction (electricity and H_2) IGCC power plant with physical absorption (Selexol)-based CO_2 capture technology. The study examined the effect of using different feed stocks such as coal, sawdust, municipal solid waste, and food waste (meat and bone) on the power output. Later, Cormos[11] compared different types of gasifiers using only coal as fuel and investigated the energy integration aspects in detail to optimize the overall plant efficiency of a coproduction IGCC plant with CCS. The study concludes that an entrained flow gasifier with dry feed and syngas heat recovery is a more promising concept than slurry feed and water quench design. Further work by Cormos[12] presented a detailed methodology to assess the performance of an iron-based CLC system using critical design factors such as gasifier selection, gasifier feeding system, and overall energy efficiency. This work suggested that a CLC-based system has a low energy penalty compared to liquid absorption process for CO_2 capture.

Li and Fan[13] addressed the energy conversion efficiencies for the chemical looping based coal conversion process. Their study shows that efficiencies of syngas chemical looping process is comparable with the current coal conversion processes for electricity and H_2 generation and could be considered as a retrofit technology in the downstream of the present gasification processes. On the other hand, they found that coal direct chemical looping combustion (CDCLC) process is more energy efficient than coal gasification based CLC process.

In addition to the investigations on energy efficiency, there are a few studies on the exergetic efficiency of various CO_2 capture technologies with combined electricity and H_2 production. Exergy analysis combines the first and second laws of thermodynamics to identify the irreversibility and losses related to each unit or process of a system. For instance, Kunze, et al.[14] presented the exergy analysis of an IGCC process by dividing the plant into three sections, the gasifier, gas treatment, and combined cycle. The analysis shows that 60% of the exergy is lost in the overall process; out of which, 31.1% is lost only in the combined cycle section, making it the most inefficient part of the process, followed by 17.1% in gas treating and 11.3% in the gasifier. Wang et al.[15] computed the exergy penalty for CO_2 capture in an IGCC process. Further, Anheden and Svedberg[16] showed the exergy analysis of CLC system with different fuels and oxygen carriers (OCs). Their results indicate that efficiency of a CLC system is similar or higher than that of a conventional combustion process.

While the existing studies have provided useful evaluation of a range of power (and in some cases H_2) generation schemes with or without CCS, their assumptions and considerations vary with respect to factors such as feedstock, power generation technology, CCS technology, production scale, and modeling approaches adopted, making it difficult to compare their results. To address this deficiency, our work uses a single basis of analysis in terms of the feedstock type, production scale, and modeling assumptions. This makes it easier and more straightforward to compare various gasification-coupled coal power plants with and without the CCS producing electricity and possibly H_2. This work provides a methodology to assess different CO_2 capture technologies based on mainly energy, exergy, and CO_2 capture efficiencies. The processes evaluated here include (i) IGCC for power generation without CCS, (ii) IGCC for power (and H_2) generation with two different precombustion CCS options based on physical absorption and adsorption, and (iii) power (and H_2) generation with CLC. Comparison is also made on the basis of the effect of ASU and GT unit integration for each of the three capture technologies. The effect of different operating conditions such as air reactor temperature and water cooling of the air reactor in the CLC process on the net electrical efficiency is another distinct feature of the present work. The findings of this work evaluate the suitability of physical absorption, physical adsorption, and CLC based CO_2 capture technologies for coal power plants by indicating the differences in overall plant performance with each type of capture technology. This article also predicts the behavior of the CLC process at different operating conditions (as stated above), which can be useful in pilot scale experimental studies.

A literature review of advanced CCS technologies has been first carried out to gather information on technical inputs and parameters such as the component flow rates, temperature, pressure, and efficiencies for various units, required for process modeling. The chemical process simulation tool Aspen Plus,

was used to develop the flowsheet models for seven different coal gasification based power plant configurations at a nominal power output of up to 467 MW. The electricity generation, H_2 production, CO_2 emission and other performance indicators such as energy and exergy efficiencies are subsequently analyzed.

2. METHODOLOGY

2.1. Process Description. Seven different types of coal gasification based power plant configurations, with and without CO_2 capture, at a power output between 141 and 467 MW have been considered. A brief description of each process is given in Table 2. The chemical process simulation tool Aspen Plus was used to develop and simulate a process flowsheet for each case. The base case (case 0) considered in this work is an IGCC plant producing only electricity without any CO_2 capture. The flowsheets for cases 1−4 are conventional IGCC process with precombustion based CO_2 capture and cases 5−6 are gasification-coupled CLC process for CO_2 capture. Cases 1, 2, and 5 generate electricity only while the cases 3, 4, and 6 produce both electricity and H_2. A stand-alone ASU generating 95% pure O_2 has been used in all seven cases, followed by an O_2-blown entrained flow shell gasifier operating at 30 atm, and fuel conversion ratio of 99.9%.[11] The power consumption by the ASU is assumed to be 225 kWh/tonne of O_2 produced.[11] The dry pulverized coal (100 μm in size) is pressurized in a lock hopper and fed to the gasifier vessel along with O_2 from the top. The coal is partially oxidized by O_2 in the gasifier to produce syngas, which mainly consists of CO and H_2. The exothermic nature of the partial oxidation reaction of coal inside the gasifier provides the heat to achieve and maintain the desired temperature of 1300 °C which is above the melting point of ash.[8] The excess heat generated in the gasifier is removed by the generation of high pressure (HP) steam. The slag in liquid form flows down the walls and comes out at the bottom with syngas. The syngas can be either quenched with water or cooled in radiative and convective heat exchanger.[8] Water quenching degrades the thermal energy of the hot syngas stream. Therefore, in our study, the syngas from the gasifier is cooled in a heat exchanger, which allows production of HP steam.

Table 2. Description of Different Cases Used in the Study

case no.	CO_2 capture technology used	electricity production	H_2 production
0 (base case)	without CO_2 capture	yes	no
1	physical adsorption (PSA)	yes	no
2	physical absorption (Selexol)	yes	no
3	physical adsorption (PSA)	yes	yes
4	physical absorption (Selexol)	yes	yes
5	CLC	yes	no
6	CLC	yes	yes

2.1.1. IGCC with Precombustion Based CO_2 Capture. This section describes the configuration of cases 1 to 4, which use PSA and Selexol technologies for CO_2 capture. First, an IGCC process producing only electricity with PSA technology for CO_2 capture (case 1), shown in Figure 1a, was developed. The detailed process flow diagram of case 1 can be seen in Supporting Information (SI) Figure S.1. In this process, the hot syngas stream at 1300 °C from the gasifier is cooled to 350 °C in a convective heat exchanger in the heat recovery steam generation (HRSG) unit where HP water used for cooling is converted into a HP steam. The cooled syngas at 350 °C is sent to two water−gas shift reactors (WGS-1 and WGS-2) aligned in series operating at temperatures 350 and 178 °C, respectively.[17,18] The WGS-1 reactor is supplied with steam at 30 atm and 350 °C generated in the HRSG. The CO in the syngas stream is partially converted to CO_2 by the steam in WGS-1 reactor generating more H_2 in the syngas. The syngas and steam exiting the WGS-1 reactor at 350 °C are cooled to 178 °C before both are fed to the WGS-2 reactor where up to 98% of the remaining CO is converted to CO_2.[19] The heat released by the cooling of syngas from 350 to 178 °C is used for preheating the boiler feedwater in the HRSG. The conversion of CO into CO_2 in the WGS reactors is an exothermic process which needs continuous removal of the excess heat to maintain the required reaction temperatures. Pressurised boiler feedwater is used as the coolant in the two WGS reactors. The syngas exiting the WGS-2 reactor at 178 °C is further cooled to 35 °C in the HRSG which condenses the steam and removes it before the syngas is sent to an acid gas removal (AGR) unit or a Selexol unit to remove sulfur; here nearly 99.9% of the hydrogen sulphide (H_2S) is stripped from the syngas using Selexol (dimethyl ether of polyethylene glycol).[12] The sulfur removed from the syngas in the form of H_2S could be converted into elementary sulfur in a Claus plant.[20] The Selexol in the sulfur removal unit is regenerated by heating which removes the dissolved sulfur and CO_2. After removing sulfur, the syngas stream is passed through the PSA-CO_2 unit where CO_2 is adsorbed by the adsorbent material (activated carbon) and the remaining gases (Tail gas−1; see Figure 1a) exits with a pressure drop of 0.49 atm.[21,22] The CO_2 separation efficiency of the PSA unit is assumed to be between 90% and 95%.[21] The adsorbent material in the PSA-CO_2 chamber is regenerated by lowering the pressure to nearly atmospheric pressure level to release CO_2.[21,22] The released CO_2 is then compressed to 150 atm for transportation and storage.[23] Case 1 does not produce any H_2, and therefore H_2-rich Tail gas-1 follows route II (as seen in Figure 1a), which is then supplied to the combustor of the GT unit after reheated to 350 °C. The high temperature exhaust gases from the GT are cooled in the HRSG unit before it is finally released to the atmosphere. The syngas and flue gas stream temperatures for case 1 are noted in SI Table S.1. The HP steam generated at 600 °C in the overall process (gasifier, heat exchangers, HRSG) is expanded through the HP, intermediate pressure (IP) and low pressure (LP) steam turbines. The exhaust steam from the HP and IP steam turbines are reheated to 600 °C before further expansion through the IP and LP turbines. The details of water and steam cycle as well as the temperature and mass flow rate of steam and water for case 1 are provided in the SI Section S.1 and Table S.2, respectively.

Case 2, which uses a Selexol-based physical absorption CO_2 capture unit (also known as acid gas removal or AGR unit) instead of a PSA-CO_2 unit after sulfur removal, is shown in Figure 1b. In this process, the outgoing gas stream from the sulfur removal unit, containing mainly CO_2 and H_2, is passed through the AGR-CO_2 unit which separates CO_2 from rest of the gases. The Selexol is regenerated by reducing the pressure to atmospheric level which releases the absorbed CO_2.[8] The CO_2 is then compressed to up to 150 atm after condensing any vapor present in the stream. After CO_2 removal, the remaining gases (Tail gas-1) are used in the GT unit as in case 1, following route II.

Case 3, which is shown in Figure 1a, is a variant of case 1, with combined electricity and H_2 production. The stream from PSA-CO_2 enters PSA-H_2 installed for H_2 separation, following route I instead of route II. A 99.99% pure stream of H_2 exits the PSA-H_2 unit after 0.49 atm of pressure drop.[8] The separation efficiency for H_2 in the PSA-H_2 unit is assumed to be 85%.[8,10] The output H_2 stream is compressed to 60 atm for transportation and storage.[8] The leftover gas (Tail gas-2) after H_2 separation leaves PSA-H_2 at nearly atmospheric pressure; hence, it needs to be compressed to the GT combustor pressure (21 atm). If more electrical energy is required, some amount of separated pure H_2 can be purged to the GT combustor according to the requirement. The remaining pure H_2 stream is compressed to 60 atm for storage. The high temperature GT exhaust is passed through the HRSG to produce HP steam and for steam reheating. Case 4, shown in Figure 1b, has an AGR-CO_2 unit for CO_2 removal instead of a PSA-CO_2 unit used in case 3. Apart from this difference, the rest of the downstream path after CO_2 removal is same as described above for case 3, which is following route I instead of route II.

2.1.2. CLC-Based Processes. A CLC process is based on transferring oxygen to the fuel from air or steam by means of a OC. An OC could be made of metal or synthetic material that is capable of carrying

dx.doi.org/10.1021/ef4024299 | Energy Fuels 2014, 28, 1028−1040

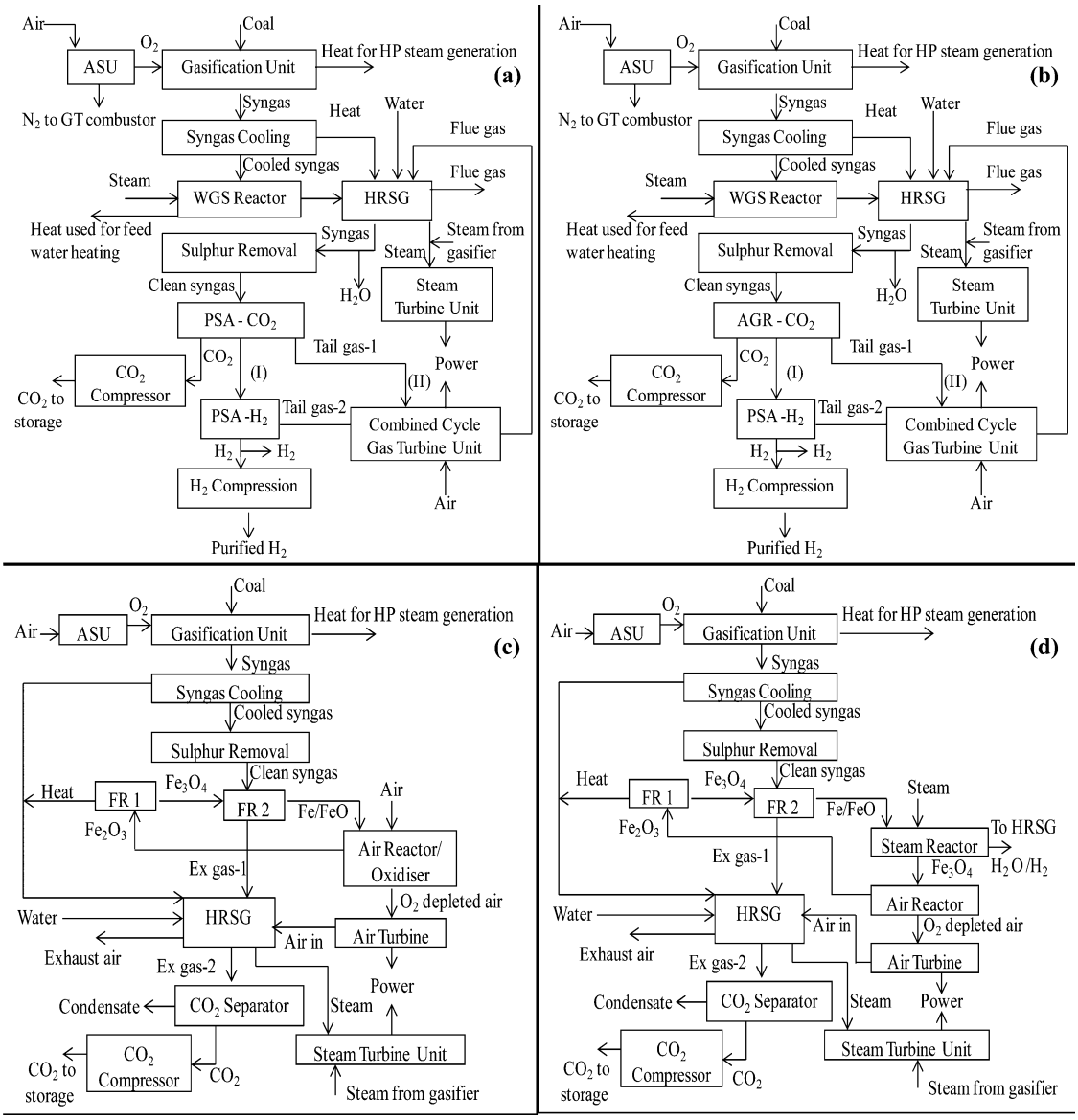

Figure 1. Simplified block flow diagrams of coal gasification-based power plant: (a) IGCC with PSA based CO_2 capture technology (cases 1 and 3); (b) IGCC with selexol based CO_2 capture (cases 2 and 4); (c) gasification-coupled CLC based CO_2 capture producing electricity only (case 5); (d) gasification-coupled CLC based CO_2 capture producing combined electricity and H_2 (case 6).

oxygen and has excellent mechanical properties to withstand attrition, agglomeration and physical stress of recycling at high temperatures. This work assumes hematite (Fe_2O_3) as the OC, supported with 15% aluminum oxide (Al_2O_3) and 15% silicon carbide (SiC) to enhance its mechanical and physical properties.[24] Parts c and d of Figure 1 show the block diagram of cases 5 and 6, respectively. In cases 5 and 6, the syngas from the coal gasifier is cooled to 35 °C in HRSG and supplied to a Selexol based sulfur removal unit. The syngas is then sent to a fluidized bed fuel reactor of the CLC process (after reheated to 350 °C) represented by two fuel reactors, FR 1 and FR 2 (see Figure 1c, d).[25] In the fuel reactors, H_2 and CO are oxidized into H_2O and CO_2 after coming in contact with Fe_2O_3. The Fe_2O_3 is first partially reduced to magnetite (Fe_3O_4) in FR 1 and then completely reduced to wustite ($Fe_{0.947}O$) in FR 2,[12,25] as shown in Figure 1c and d. A cyclone separator removes the reduced OC particles from the hot gases coming out of the FR 2. These hot gases are cooled in a HRSG unit to condense the water vapor and produce a pure stream of CO_2, which is compressed to 150 atm for storage. The sensible heat lost by the hot gases from the CLC fuel reactor is used to generate HP steam and for steam reheating. In case 5, the reduced OC particles ($Fe_{0.947}O$) are fully regenerated to Fe_2O_3 in the air reactor where they are oxidized by pressurized air, which also helps in circulation of OC in the system. The oxidation of $Fe_{0.947}O$ by air is a highly exothermic process. The air reactor is maintained at 1300 °C by supplying excess air than usually required for OC regeneration.[26] The hot pressurized air exiting the air reactor is separated from the OC particles in a cyclone separator and expanded in an air turbine. The regenerated OC particles are recycled back to the FR 1. The air turbine exhaust has a high temperature and, therefore, is sent to the HRSG unit for heat recovery before released to the atmosphere. The steam generated in the whole process (i.e., gasifier, CLC reactors, HRSG and other heat exchangers) is used to drive the HP, IP, and LP steam turbines. As in cases without CLC, the exhaust steam from the HP and IP steam turbines is reheated in the HRSG unit to 600 °C before expanding through IP and LP steam turbines.

In case 6, the reduced OC from the fuel reactors is partially oxidized to Fe_3O_4 in the steam reactor using steam at 30 atm and 350 °C generated in the HRSG unit. This oxidation reaction of the OC is an exothermic process that generates H_2, which with some steam and OC particles comes out from the exhaust of the steam reactor maintained at 550 °C through HP water/steam cooling. The OC particles are separated from the steam and H_2 in a cyclone separator and sent for

dx.doi.org/10.1021/ef4024299 | Energy Fuels 2014, 28, 1028−1040

complete oxidation to Fe_2O_3 by compressed air (which is again an exothermic reaction) in an air reactor (see Figure 1d). The hot mixture of H_2 and steam after OC separation is cooled in HRSG unit that causes the steam to condense, generating a pure stream of pressurized H_2 for further compression to 60 atm and storage. The hot pressurized air from the air reactor is expanded in an air turbine and then supplied to the HRSG unit before it is finally released to the atmosphere. Equations 1 to 7 represent the reactions taking place inside the reactors of a CLC process using an iron based OC.

Fuel Reactor.

$$CO + Fe_2O_3 \rightarrow CO_2 + 2Fe_{0.947}O \quad (1)$$

$$H_2 + Fe_2O_3 \rightarrow H_2O + 2Fe_{0.947}O \quad (2)$$

Air Reactor. For case 5,

$$2Fe_{0.947}O + \frac{1}{2}O_2 \rightarrow Fe_2O_3 \quad (3)$$

For case 6,

$$2Fe_3O_4 + \frac{1}{2}O_2 \rightarrow 3Fe_2O_3 \quad (4)$$

Steam Reactor. (case 6 Only)

$$2Fe_{0.947}O + H_2O \rightarrow Fe_2O_3 + H_2 \quad (5)$$

Net Reaction. For case 5,

$$CO + H_2 + O_2 \rightarrow CO_2 + H_2O \quad (6)$$

For case 6,

$$CO + H_2 + \frac{1}{2}O_2 + H_2O \rightarrow CO_2 + H_2O + H_2 \quad (7)$$

2.2. Modeling Assumption and Simulation. The key modeling information and choices used in the simulations are shown in Tables 3 and 4. Table 3 shows the physical and chemical properties of Illinois #6 type coal used as fuel in all the cases. The stream class from Aspen Plus used in all cases is MIXCINC. The databanks selected for Aspen Plus simulations are COMBUST, INORGANIC, SOLIDS, and PURE22.[24,27] The PR-BM property method is adopted for conventional components.[24] Coal and ash used in the simulation models are

Table 3. Physical and Chemical Properties of Illinois #6 Coal[27,41]

Proximity Analysis		
items	weight as received (%)	dry weight (%)
moisture	11.12	
fixed carbon	44.19	49.72
volatiles	34.99	39.37
ash	9.70	10.91
total	100.00	100.00
HHV(MJ/kg)	27.13	30.53
Ultimate Analysis		
moisture	11.12	
ash	9.70	10.91
carbon	63.75	71.72
H_2	4.5	5.06
N_2	1.25	1.41
chlorine	0.29	0.33
sulfur	2.51	2.82
O_2	6.88	7.75
Sulfate Analysis		
pyritic		1.70
sulfate		0.02
organic		1.10

Table 4. Design Assumptions Used for Developing the Process Flowsheets for CO_2 Capture Cases[8,11,17−19,21,22,26,42]

unit	case 1	case 3	case 2	case 4	case 5	case 6
ASU and compressors	Oxygen purity: 95% (by mass). ASU O_2 and N_2 delivery pressure: 2.67 atm. Air compressor pressure: 7 atm. O_2 compressor pressure: 36 atm. Compressor efficiency: 83%					
gasification reactor	Pressure: 30 atm. Temperature: 1300 °C. Oxygen/coal ration (kg/kg): 0.867. Carbon conversion: 99.9%					
WGS reactor	Pressure: 30 atm. Temperature: Reactor 1 350 °C and Reactor 2 178 °C. CO conversion: 98%. Steam/CO ratio: 0.698					
air reactor					Temperature: 900 to 1300 °C. Pressure: 30 atm	
steam reactor					Temperature: 550 °C. Pressure: 30 atm	
fuel reactor					Temperature: 700 to 1121 °C. Pressure: 30 atm	
sulfur removal	Selexol based physical absorption method; H_2S removal yield: 99.9%					
H_2 removal and compression		PSA; Separation efficiency: 85%. Multistage compressor. Compression pressure: 60 atm.		PSA; Separation efficiency: 85%. Multistage compressor. Compression pressure: 60 atm.		Multistage compressor. Compression pressure: 60 atm.
CO_2 removal and compression	PSA; CO_2 removal yield: 90−95%. Adsorbent material used is activated carbon. Multistage compressor outlet pressure: 150 atm.		Selexol process (AGR); CO_2 removal yield: 95%. Multistage compressor outlet pressure: 150 atm.		CO_2 removal yield: 99.9%. Multistage compressor Outlet pressure: 150 atm.	
GT unit	Isentropic efficiency: 88%. Discharge pressure: 1.05 atm. Inlet temperature: 1300 °C (for cases 0−2, 5), 1150−1250 °C (for cases 3, 4), and 650−750 °C for case 6.					
steam turbine unit	Three level pressures (HP/IP/LP): 124/30/6.5 bar. Isentropic efficiency: 86%. Condenser pressure: 0.046 bar.					

dx.doi.org/10.1021/ef4024299 | *Energy Fuels* 2014, 28, 1028−1040

considered as nonconventional components; therefore, information about their physical and chemical properties is needed. The property methods used for coal and ash are HCOALGEN and DCOALIGT, respectively.[28] The OC and support materials are entered as solid in the component input data in Aspen Plus. The Barin equation is used to calculate the physical properties of the solid compounds.[24] The model retrieves the CPSXP (a−h) coefficients from the INORGANIC databank of Aspen.[24]

The key conditions and input parameters of each process unit such as gasifier, ASU, turbines, and reactors are presented in Table 4. In all the seven processes studied in this work, the raw syngas is produced in a conventional gasification process represented by a RYILED decomposer and a RGIBBS gasifier unit. A detailed description of reactor modeling is given in Section 2.3. Four-stage adiabatic compressors represented by the MCOMPR model in Aspen Plus, are used for gas compression. These compressors need the discharge pressure from the final stage and isentropic efficiency as the input to the Aspen Plus model. The Aspen Plus PUMP models with an isentropic efficiency of 90% have been used to simulate pressurization of the water needed for steam generation. For heat recovery steam generation (HRSG), MHeatX type counter current heat exchangers are used.

2.3. Reactor Modeling for the CLC Process. This section describes the reactor models used in the simulations. The built-in Aspen Plus reactor models RYIELD and RGIBBS are used to design different reactive processes including (i) gasification, (ii) WGS reaction, (iii) oxidation of fuel in fuel reactor, and (iv) OC regeneration in steam and air reactor.

2.3.1. Gasification. A dry feed type entrained flow shell gasifier is considered in this work due to its dominance in the commercial IGCC plant designs. An RYIELD reactor block is used to decompose the pulverized coal powder into its conventional constituent elements and also calculates the heat required for it. RYIELD reactors are used where inlets are unknown and the outlets known. The conventional elements provided after decomposition of coal are fed to the RGIBBS reactor block, which determines the possible products and their composition at equilibrium conditions. The RGIBBS reactor is an equilibrium based reactor, which restricts individual equations to equilibrium and does not take account of the reaction kinetics. This type of reactor considers all the components as possible products, which is useful when there are many reactions between several components and the reaction kinetics is unknown. The operating temperature, pressure and O_2 to coal ratio are the key parameters required as input to the RGIBBS reactor.

2.3.2. WGS Reactor. A two stage WGS reaction has been considered in cases 1−4. These reactors are supplied with hot syngas and steam at 30 atm at 350 and 178 °C, respectively. A WGS reactor is modeled by using a REquil block, which is an equilibrium based reactor in Aspen Plus. This block is useful when there are few reactions and the reaction kinetics is unknown. It combines the chemical and phase equilibrium to generate the products of reaction. The temperature, pressure, and the chemical reaction equations are the key parameters required as input to a REquil reactor.

2.3.3. CLC Fuel Reactor. The reactants and products of the CLC fuel reactors are assumed to be well-mixed. Simple RGIBBS reactor blocks of Aspen Plus are used for the simulation of the CLC fuel oxidization process under equilibrium conditions. The operating temperature, pressure, and molar flow of OC particles and syngas are the key input parameters required for this model. The temperature and pressure are considered to remain constant. The reactions taking place inside the fuel reactors are endothermic and require heat, which is provided by high temperature OC particles (Fe_2O_3) supplied from the air reactor.

2.3.4. CLC Steam and Air Reactor. The steam reactor of a CLC system uses steam to partially oxidize the reduced OC particles to Fe_3O_4 while generating H_2 as a product at thermodynamic equilibrium. The H_2 yield of the steam reactor is directly proportional to the OC conversion. The steam reactor was modeled in Aspen Plus by using a single RGIBBS reactor block. The key operating parameters used for modeling the steam reactor are operating temperature, pressure and molar flow ratio between steam and OC. The air reactor effected complete oxidization of the reduced OC particles to Fe_2O_3 and was modeled as an entrained bed reactor with air and OC particles flowing cocurrently through the vessel. The combustor model, operating at a constant temperature and pressure, was used to predict the excess heat produced and the possible products. All of the combustion reactions are assumed to be fully completed in the combustor and this was sufficiently modeled using a RGIBBS model. The ratio between OC and air supplied and the operating temperature are the key variables for the air reactor model.

2.4. Plant Performance Indicators. All cases were evaluated from both the energy and exergy point of view. The assessment of the overall performance of all the processes was performed using streamflow data, for example, mass flow of the components, pressure, temperature, power, and energy output provided by the simulation of each process configuration. The terms discussed below are used as the key plant performance indicators.[11,12]

Gross electrical efficiency (η_{gross}) indicates the overall electricity produced by the steam and gas turbines used in the process. It does not consider the energy consumed by the auxiliary elements needed to run the plant and can be calculated using eq 8.

$$\eta_{gross} = \frac{\text{Gross power output } (MW_e)}{\text{Feed stock LHV } (MW_{th})} \times 100 \quad (8)$$

Net electrical efficiency (η_{net}) shows the actual electrical power produced by the system. This is calculated by deducting all the auxiliary energy consumed from the gross electricity produced, as shown in eq 9.

$$\eta_{net} = \{[\text{Gross power output } (MW_e) - \text{Auxiliary energy consumed } (MW_e)]/[\text{Feed stock LHV } (MW_{th})]\} \times 100 \quad (9)$$

H_2 energy efficiency (η_{H_2}) applies to cases 3, 4, and 6 which produce both H_2 and electricity. The term indicates the efficiency of the system in producing H_2 from the coal feed. The thermal energy of H_2 is used to calculate H_2 efficiency, as shown by eq 10.

$$\eta_{H_2} = \frac{\text{Hydrogen thermal energy } (MW_{th})}{\text{Feed stock thermal energy } (MW_{the})} \times 100 \quad (10)$$

Overall energy efficiency ($\eta_{Overall}$) for cases 1, 2, and 5 producing only electricity is the same as the net electrical efficiency shown by eq 9. For the cases 3, 4, and 6, $\eta_{Overall}$ is calculated by adding both electrical and H_2 energy efficiency as shown by eq 11.

$$\eta_{Overall} = \eta_{net} + \eta_{H_2} \quad (11)$$

Specific CO_2 emission (SE_{CO_2}) gives the amount of CO_2 released to the atmosphere by the system for per MW of energy generated, which is equal to the net electrical energy output for cases producing only net electricity, and electrical plus thermal energy of H_2 for cases with coproduction. SE_{CO2} is calculated by eq 12.

$$SE_{CO_2} = \frac{\text{emitted } CO_2 \text{mass flow (t/h)}}{\text{net power output } (MW_e) + \text{hydrogen energy } (MW_{th})} \quad (12)$$

2.4.1. Exergy Analysis. Exergy is the maximum work that can be extracted from a system interacting with a reference environment, which is taken as 1 atm and 25 °C for this study.[29] For a process stream, its exergy can be divided into two parts (physical and chemical).

Physical exergy (Ex_{ph}) equals to the maximum reversible amount of work obtainable when a stream of substance is brought from its actual state to the environmental state. The physical processes involve only thermal and mechanical interaction with the environment which is defined by pressure P_0 and temperature T_0, respectively.[30] Assuming that potential and kinetic energy can be neglected, the physical exergy is expressed by eq 13:

$$\mathrm{Ex}_{ph} = (h - h_0) - T_0(s - s_0) \quad (13)$$

where h and s are specific molar enthalpy (kJ/kmol) and specific molar entropy (kJ/kmol K), respectively; h_0 and S_0 are the values of h and s at standard conditions (T_0, P_0).

Chemical exergy (Ex_{ch}) of a substance is the maximum amount of work obtainable by bringing it from the environmental state (T_0, P_0) to a full equilibrium with the chosen environment. The molar chemical exergy of an ideal mixture is expressed by eq 14 as

$$\mathrm{Ex}_{ch_{total}} = \sum_i x_i \mathrm{Ex}_{ch_i} + RT_0 \sum_i x_i \ln x_i \quad (14)$$

where x_i and Ex_{ch_i} are molar fraction and molar chemical exergy (kJ/kmol), respectively, of each component in the mixture, and R is the universal gas constant.

Exergy loss (Ex_{loss}) of each individual unit can be calculated by finding the difference between the exergy of input and output streams of this unit:

$$\mathrm{Ex}_{loss} = \mathrm{Ex}_{total_{in}} - \mathrm{Ex}_{total_{out}} \quad (15)$$

Total exergy (Ex_{total}) of stream is taken as the sum of its physical and chemical exergy:

$$\mathrm{Ex}_{total} = \mathrm{Ex}_{ph} + \mathrm{Ex}_{ch} \quad (16)$$

Chemical exergy of coal (Ex_{coal}): In calculation of the total exergy of coal, its physical exergy is considered to be zero, because the input coal feed is in the physical equilibrium with the environment. The chemical exergy of coal can be estimated using eqs 17 and 18. These equations are only applicable when the oxygen to carbon ratio in the given coal feed is less than 0.667.[31]

$$\mathrm{Ex}_{ch_{coal}} = (\mathrm{CV} + wh_{fg})\varphi_{dry} + 9417s \quad (17)$$

CV is the net calorific value of Illinois # 6 type coal in kJ/kg, w is the percentage of moisture content in the coal, h_{fg} is the latent heat of water in kJ/kg at temperature, T_o, and s denotes the mass fraction of sulfur in the fuel. The term φ_{dry} is be calculated by using the eq 18.

$$\varphi_{dry} = 0.1882\frac{h}{c} + 0.061\frac{o}{c} + 0.0404\frac{n}{c} + 1.0437 \quad (18)$$

where c, h, o, and n represents the mass fractions of carbon, hydrogen, oxygen, and nitrogen in the coal feed, respectively.

H_2 exergy efficiency ($\eta_{\mathrm{Ex}_{H_2}}$) is taken as the ratio of the total exergy content in H_2 product to the chemical exergy of the coal feed:

$$\eta_{\mathrm{ExH}_2} = \frac{\text{overall exergy in } \mathrm{H}_2\ (\mathrm{MW}_{th})}{\text{chemical exergy in coal feed } (\mathrm{MW}_{the})} \times 100 \quad (19)$$

Exergy efficiency (η_{ex}) of a system is the ratio of total exergy output to the total exergy given to the system. For the cases considered in this study, the total exergy output is the sum of electrical work output and chemical exergy of H_2 stream produced in the process whereas the chemical exergy of the coal feed is taken as the exergy input to the system, as shown in eqs 20 and 21:

$$\eta_{ex} = \frac{\text{Total exergy output of the system}}{\text{Total exergy given to the system}} \times 100 \quad (20)$$

$$\eta_{ex} = \frac{\text{Net electrical energy} + \text{total } \mathrm{H}_2 \text{ exergy } (\mathrm{MW}_{e+th})}{\text{Total chemical exergy in feed stock } (\mathrm{MW}_{the})} \times 100 \quad (21)$$

3. RESULTS AND DISCUSSIONS

3.1. Comparison of CLC Process with Physical Absorption and Adsorption Processes for Only Electricity Generation Cases. The net electrical efficiency and CO_2 captured shown in Tables 5 and 6 are the two main investigated parameters, which are discussed in this section to compare CLC, PSA, and Selexol based capture technologies. The simulation results of the CLC process that produces only electricity (case 5) give an overall electrical efficiency of 38.7%, which is close to what is observed by a previous study.[32] The PSA (case 1) and Selexol (case 2) based processes showed an overall electrical efficiency of 37.4 and 36.4%, respectively, which is lower than case 5. The electrical efficiency achieved for case 5 is also found to be substantially higher as compared with amine-based postcombustion capture technology, which has efficiency between 26.7 and 35.3%.[33] The overall CO_2 capture efficiency of the CLC process is 99.9% compared with 89.9% for PSA and 93.5% for Selexol processes. This lower overall capture efficiency of PSA and Selexol process is mainly due to the following reasons: (i) the 98% CO conversion efficiency of

Table 5. Plant Performance Indicators for Cases Producing Electricity Only

plant data	units	case 0	case 1	case 2	case 5
fuel input energy, LHV (A)	MW_{th}	1126.5	1126.5	1126.5	1126.5
net GT output	MWe	319.7	301.2	296.2	259.9
steam turbine output	MWe	224.7	223.8	221.8	269.8
gross electric power output (B)	MWe	544.4	525.0	518.0	529.7
ASU consumption + O_2 compression	MWe	34.1	34.1	34.1	34.1
CO_2 capture and compression	MWe		26.3	29.9	10.2
power cycle pumps	MWe	3.0	3.0	3.9	3.52
other	MWe	40.5	40.5	40.5	45.0
total ancillary power consumption (C)	MWe	77.6	103.9	108.4	92.8
net electric power output (D) (D = B − C)	MWe	466.8	421.1	409.6	436.9
gross electrical efficiency (B/A × 100)	%	48.3	47.3	46.7	47.0
net electrical efficiency (D/A × 100)	%	41.4	37.4	36.4	38.7
overall energy produced (electricity)	MWe	466.8	421.1	409.6	436.9
overall plant energetic efficiency	%	41.4	37.4	36.4	38.7
overall plant exergetic efficiency	%	37.2	33.5	32.6	34.6
CO_2 capture efficiency	%		89.9	93.5	99.9
exergy in captured CO_2 stream (% fuel chemical exergy)	%		7.5	7.9	10.2
overall exergy considering exergy of captured CO_2 stream	%		41.0	40.5	44.4
CO_2 emission	t/h	278.3	33.6	21.1	0.28
CO_2 specific emissions	t/MWh	0.597	0.079	0.051	0.0006
CO_2 captured	t/h		244.7	257.2	278.0
CO_2 captured (specific)	t/MWh		0.581	0.627	0.63

Table 6. Amount of CO_2 Captured Per Unit Energy and Efficiency Penalty for Cases 1, 2, and 5 with Reference to the Base Case

plant data	unit	case 1	case 2	case 5
CO_2 captured per MW decrease in energy production than the base case	t/h	5.3	4.5	9.3
net electrical efficiency penalty	%	4.0	5.0	2.7
relative decrease in net electrical efficiency compared to the base case	%	9.6	12.0	6.5
CO_2 captured per unit decrease in net electrical efficiency from base case	t/h	61.1	51.4	102.9

dx.doi.org/10.1021/ef4024299 | Energy Fuels 2014, 28, 1028−1040

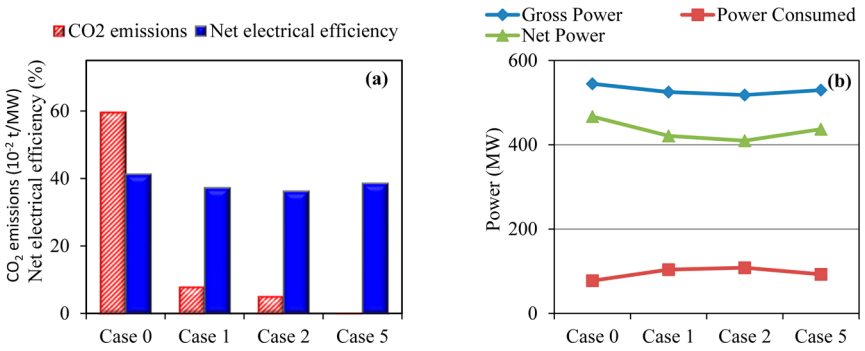

Figure 2. (a) Relation between electricity production and CO_2 emissions for cases 0, 1, 2, and 5 and (b) relation between power production, power consumption and net power output for cases 0, 1, 2, and 5.

WGS reactors compared to 99.99% conversion in the CLC fuel reactor and (ii) 90.3% CO_2 capture efficiency for the PSA and 95.0% for Selexol units, compared to the assumed complete capture by CLC. The unconverted CO from the WGS reactor is oxidized in a combustor after the CO_2 removal step in the presence of air to produce CO_2. This CO_2 along with the uncaptured CO_2 from the CO_2 removal unit is expanded in a GT before it is finally vented to the atmosphere with the other flue gases.[8]

Figure 2a shows the variation in electricity production and carbon emissions for all the three different CO_2 capture cases with electricity production only. Compared with the CLC process (case 5) that emits 0.0006 t/MWh of CO_2 at an emission rate of 0.28 t/h, the PSA (case 1) and Selexol (case 2) technologies emit 0.079 and 0.051 t/MWh of CO_2 at an emission rate of 33.6 and 21.1 t/h, respectively. Figure 2b shows a comparison between cases 0, 1, 2, and 5 for gross power output, power consumption, and net power produced. CLC process (case 5) produces less power from the GT unit, but it generates more power from the steam turbines, which results in more net electricity production (436.9 MW) compared with case 1 (421.1 MW) and case 2 (409.6 MW).

3.2. Comparison of CO_2 Capture Cases (Cases 1, 2, and 5) Producing Only Electricity with the Base Case (Case 0). Table 5 shows the results of case 0, which is taken as a base case that produces only electricity without any CO_2 capture. In case 0, the syngas stream from the WGS reactors is supplied to the combustor unit eliminating the CO_2 scrubbing step. The unconverted CO, and H_2 from the WGS reactor unit are oxidized in the combustor in the presence of air. The product stream from the combustor is expanded through the GT and sent to HRSG before it is finally vented to the atmosphere. The base case has a higher net electrical efficiency of 41.4% compared to the other cases (cases 1, 2, and 5), which produce only electricity with CO_2 capture. Figure 3 shows that case 2 using the Selexol process suffers the highest net energy penalty of 57.2 MW versus case 0 compared to 29.9 MW for CLC and 45.7 MW for PSA-based processes. The results from Table 6 indicate that per MW decrease in energy production compared to the base case, the CLC process captures significantly higher CO_2 (9.3 t/h) compared to PSA (5.3t/h) and Selexol (4.5 t/h) process. The relative decrease in the net electrical efficiency in comparison to base case (case 0) for precombustion based capture processes (case 1 and 2) is lower than the energy penalty of 20−29% for the amine based postcombustion capture methods described in a report of the IEA.[33]

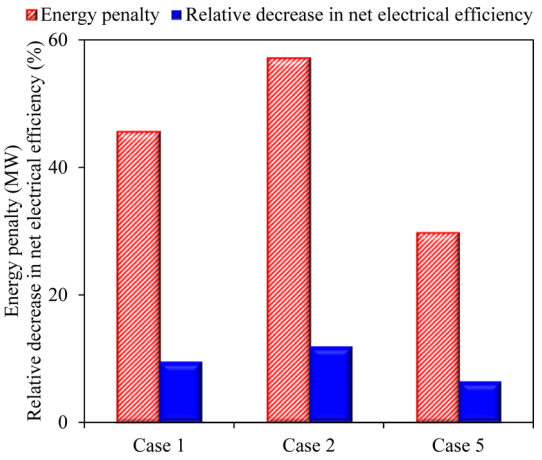

Figure 3. Energy and efficiency penalty in cases 1, 2, and 5 with reference to the case 0.

3.3. Energy Consumption in CO_2 Compression for Cases 1, 2, and 5. Table 7 shows the energy consumption in CO_2 compression work for PSA, Selexol and CLC processes. It can be seen that the CLC process (case 5) requires only 10.2 MW for compressing 278 t/h of CO_2 whereas the IGCC with PSA (case1) and IGCC with Selexol (case 2) processes require 26.3 MW and 29.9 MW, respectively, even though they compress less CO_2 compared to the CLC. This is due to the fact that the CO_2 stream available for compression in this CLC process is already at elevated pressure levels of approximately 30 atm, and therefore, less energy is required for compressing CO_2 to 150 atm. On the other hand, the CO_2 streams available for compression in the cases of the PSA and Selexol processes are very close to atmospheric pressure, which explains the higher compression energy requirement for these two technologies. Further analysis can be made to consider the CO_2 stream being produced from the system at a pressure of 1 atm. For cases 1 and 2, this would mean that the CO_2 compression step is eliminated. In case 5, this analysis assumes that the pressurized (30 atm) CO_2 stream from the fuel reactor is expanded in an expander, which will produce an extra 5.11 MW of power. As shown in Table 7, the CLC process will still be more energy efficient than the Selexol and PSA processes and attain a net electrical efficiency of 40.0%. Some consider that this analysis could be useful if the CO_2 captured from the power plant were to be used in other industries, instead of sequestration. For example, the food and chemical sectors may have no need for compressed CO_2. However, very few processes other than enhanced oil recovery (EOR) and

dx.doi.org/10.1021/ef4024299 | Energy Fuels 2014, 28, 1028−1040

Table 7. Comparison of CO_2 Compression Work for Cases 1, 2, and 5

case no.	electrical efficiency (%)	CO_2 captured (%)	CO_2 compression work (MW)	CO_2 captured (t/h)	compression work per tonne of CO_2 captured (MWh/t)	electrical efficiency with CO_2 produced at 1 atm (%)
0	41.4	0	0	0	0	41.4
1	37.4	89.9	26.3	244.7	0.107	39.7
2	36.4	93.5	29.9	257.2	0.116	39.0
5	38.7	99.9	10.2	278.02	0.036	40.0

potentially the production of urea are likely to be able to utilize a significant fraction of the CO_2 produced by a gasifier producing 467 MWe.

3.4. Comparison of CO_2 Capture Technologies for Combined Electricity and H_2 Production Cases. One of the main objectives of this work was to investigate the suitability of the gasification-coupled CLC process (case 6) compared to IGCC with PSA (case 3) and Selexol (case 4) technologies for combined electricity and H_2 generating plants. Table 8 summaries the results of these cases for identical H_2 production rates (524 MW) from each process. Case 6 with CLC yields an overall energy efficiency (59.4%), which is marginally higher than case 4 Selexol (59.1%). Case 6 has a lower overall efficiency compared to the case 3 PSA (60.0%) process owing to two main reasons: (i) lower GT inlet temperature of 727 °C compared to 1185 °C for case 3 and (ii) higher power consumption by the air compressor in air reactor.

Figure 4 shows the trade-off between the electrical, H_2 and overall efficiencies for case 6. The overall efficiency increases with the H_2 production rate whereas the electrical efficiency shows an opposite trend. The decrease in electrical power is the result of less H_2 being available for combustion in the GT combustor unit. The H_2 produced in the steam reactor of the CLC system can be used for electricity generation during periods of high electricity demand by simply burning it in a separate combustor and expanding through the GT along with the hot air reactor exhaust. This can provide flexibility to the CLC system with respect to changing loads.

Table 8. Plant Performance Indicators for Cases with Combined Electricity and H_2 Production

plant data	units	case 3	case 4	case 6
fuel input energy, LHV (A)	MW_{th}	1126.5	1126.5	1126.5
H_2 produced (LHV)	MWe	524.0	524.0	524.0
net GT output	MWe	136.2	130.9	61.5
steam turbine output	MWe	135.6	133.3	177.9
gross electric power output (B)	MWe	271.8	264.2	239.5
ASU consumption + O_2 compression	MWe	34.1	34.1	34.1
CO_2 capture and compression	MWe	26.3	29.9	10.2
H_2 compression	MWe	4.1	4.6	4.4
other	MWe	55.1	53.8	45.07
total ancillary power consumption (C)	MWe	119.6	122.4	93.7
net electricity produced	MWe	152.2	141.8	145.8
net electrical efficiency	%	13.5	12.6	12.9
H_2 efficiency	%	46.5		
overall energy produced (H_2 + electricity)	MWe	676.2	665.8	669.8
overall plant energetic efficiency	%	60.0	59.1	59.4
overall plant exergetic efficiency	%	53.6	52.7	53.0
CO_2 capture efficiency	%	89.9	93.5	99.9
exergy in captured CO_2 stream (% fuel chemical exergy)	%	7.5	7.9	10.2
overall exergy considering exergy of captured CO_2 stream	%	61.1	60.6	63.2
CO_2 emission	t/h	33.6	21.1	0.28
CO_2 specific emissions	t/MWh(e)	0.220	0.148	0.002
CO_2 specific emissions (total)	$t/MWh_{(e+th)}$	0.049	0.031	0.0004
CO_2 captured	t/h	244.7	257.2	278.0
CO_2 captured (specific)-electric	t/MWh(e)	1.60	1.81	1.90
CO_2 captured (specific)-thermal	$t/MWh_{(e+th)}$	0.36	0.38	0.41

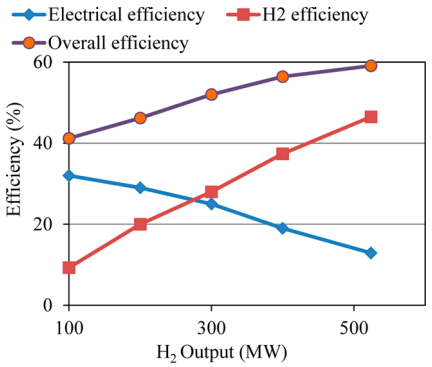

Figure 4. Variation of electrical, H_2, and overall efficiency versus the H_2 output for case 6.

3.5. Exergy Analysis of PSA, Selexol, and CLC Technologies. Tables 5 and 8 show the results of exergy analysis for all the seven cases. The study indicates an overall exergetic efficiency of 53.6% for case 3 with the PSA process producing combined electricity and H_2, which is the highest among all the seven cases analyzed here. The other two cases for electricity and H_2 production using Selexol (case 4) and CLC (case 6) process have exergetic efficiencies of 52.7 and 53.0%, respectively. The exergetic efficiency of CLC process is higher compared to Selexol and PSA processes in cases with electricity production only. It is also seen that the captured CO_2 stream contains 7.5−10.2% of the total chemical exergy of the coal used as the fuel to the system. If this exergy of the captured CO_2 stream is considered to recognize the effort dedicated to CO_2 capture, it would make the CLC process more exergetically efficient among the cases with combined H_2 and electricity production.

3.6. Effect of Using N_2 Available from ASU in GT on Power Output. All the configurations with CO_2 capture, represented by cases 1−6, assumed that N_2 from the ASU is added to the feed to the GT unit to enhance its power output. The N_2 stream produced in the ASU is compressed (22 atm for

dx.doi.org/10.1021/ef4024299 | Energy Fuels 2014, 28, 1028−1040

the cases without CLC process and 32 atm for CLC) and supplied to the combustors (in cases without CLC) and to the air reactors (in cases with CLC) eventually for expansion through the GT/air turbine. Figure 5 shows that all the

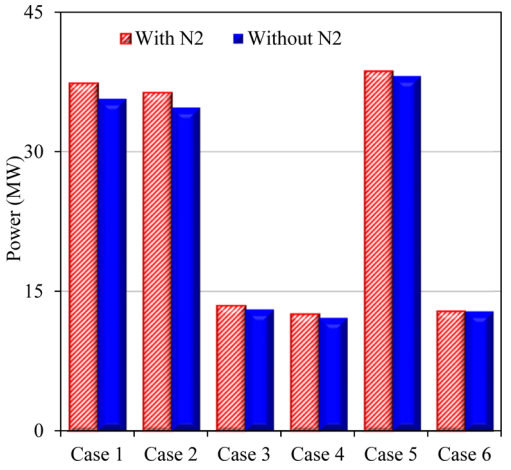

Figure 5. Effect of ASU integration on power output for cases 1−6.

processes benefit, in terms of their power output, from the integration of ASU with the GT unit. The gasification-coupled CLC process (cases 5 and 6) is least effected by ASU integration. In contrast, case 1 experiences 4.7% increase in the net electrical efficiency which is the highest among all six cases. The results show that integrating N_2 stream with the GT cycle can improve the overall electrical efficiency of the process despite the extra work required for N_2 compression.

Potentially, further integration can be done to use the air from the more efficient compressor of the GT power cycle to supply compressed air to the ASU. This type of integration can completely eliminate the low efficiency ASU compressors.[34] A GT compressor can supply HP air to the ASU. The main limitation of such integration is that the ASU cannot start unless the GT starts running. This problem can be resolved by using a separate air compressor for the ASU to start up the process.

3.7. Effect of Air Reactor Temperature on the Power Output of the CLC-Based Process. With the model of gasification-coupled CLC (case 5), the effect of change in air reactor temperature on the net electric power produced has been analyzed. Figure 6a shows that the net power production increases with the air reactor temperature. The power is produced in the GT unit, which is supplied with hot exhaust from the air reactor, and in the steam turbine unit. Steam is generated by the HRSG unit which recovers heat from the hot exhaust of the fuel reactor and that of the gas turbine. The air reactor regulates its temperature via the amount of excess air supplied to the reactor beyond what is required by complete combustion. Figure 6a shows that as the temperature of the air reactor increases, both the power from the stream turbine unit and that from the GT unit increase.

The exhaust gases from the air reactor are expanded through the GT, which gives a higher yield when operated at a higher temperature range. This provides the explanation behind the increase in GT power output with air reactor temperature. When the air reactor is maintained at higher temperature, the temperature of OC supplied to the fuel reactor from the air reactor is also high and hence is higher the fuel reactor temperature. This means a high temperature fuel reactor exhaust is available in the HRSG for steam generation, explaining the reason behind the gain in steam turbine power output with increase in air reactor temperature.

3.8. Effect of Water-Cooling of the CLC Air Reactor on the Power Output. The CLC system (case 5) was examined for the effects of using water-cooling of the air reactor instead of excess air supply as an alternative to maintain the required temperature of 1300 °C throughout the study. The HP water after absorbing heat from the air reactor is converted into HP steam, which is used for power generation. It has been found from the sensitivity analysis that an excess air supply of 81.14% can maintain the desired air reactor temperature without requiring any cooling by water. Figure 6b indicates that the use of water-cooling results in decrease in the feed to the GT, gross, and net power output of the system, whereas the steam turbine output power increase due to more steam available for the steam turbines. Completely using water/steam cooling for the air reactor can decrease the net power output by ∼5.7%. However, this can help in reducing the size of the air reactor, compressor, gas−solid separator, and GT, and hence, the capital cost of the plant.

4. SUMMARY AND CONCLUSIONS

This article investigates the performance characteristics of seven different types of gasification based coal power plants with and without the CO_2 capture using PSA, Selexol and CLC processes. Cases 0, 1, 2, and 5 produced only electricity while

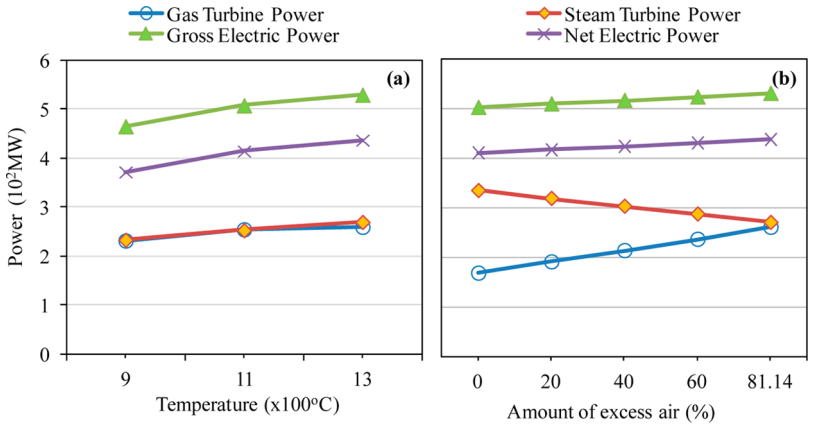

Figure 6. Effect of (a) air reactor temperature and (b) water-cooling of the air reactor on the power output for CLC process.

dx.doi.org/10.1021/ef4024299 | *Energy Fuels* 2014, 28, 1028−1040

cases 3, 4, and 6 produced combined electricity and H_2. All seven process flowsheet models were developed using a chemical process simulation tool "Aspen Plus". The results generated from the flowsheet simulation models were compared based on the electrical efficiency, H_2 production, and CO_2 emissions. The effect of ASU and GT integration on the performance of all CO_2 capture cases was estimated. Sensitivity analysis was performed for the CLC process to study the plant behavior with respect to air reactor temperature and water cooling of the air reactor.

Among the systems producing only electricity with CO_2 capture, the CLC based process achieves the highest electrical efficiency (38.7%) compared with PSA (37.4%) and Selexol (36.4%) based processes. In electricity and H_2 cogeneration cases, the CLC-based process has marginally lower (by 0.6%) and higher (by 0.3%) net electrical efficiencies than the PSA and Selexol based process, respectively. However, CLC process can capture 99.9% of CO_2 produced, which is potentially higher in comparison to 89.9% for PSA and 93.5% for Selexol based processes. Further comparison among the three capture processes could also be made, based on the cost and life cycle analysis in order to assess the combined techno-economic viability, but such a comparison is beyond the scope of our present study. The ASU and GT integration results in higher power output for all the cases; however, the cases with CLC process have the least effect. The sensitivity analyses performed on CLC process shows that it is favorable to operate the air reactor at higher temperatures for more net power output. Also it has been concluded that cooling of air reactor (while maintaining 1300 °C) by using excess air supply instead of pressurized water tends to increase the net power output of the CLC system.

In addition to the factors considered in the current work, a number of potential improvements will be studied in future investigations. These include extracting and utilizing the heat released by the intercooled compressors, and replacing the cryogenic ASU with membrane-based technology, which can possibly be more efficient when integrated with the GT unit. A detailed sensitivity analysis of the three capture technologies at all different possible operating conditions will be considered in future work to further study and understand the plant behavior in order to assist the optimization of power plants. The CLC process has comparatively more scope of efficiency improvement in future by directly using the solid coal fuel into the fuel reactor, eliminating a separate gasification and ASU, which are responsible for high exergy losses in the system.

■ ASSOCIATED CONTENT

Ⓢ Supporting Information

Detailed process flow diagram of case 1; This information is available free of charge via the Internet at http://pubs.acs.org/.

■ AUTHOR INFORMATION

Corresponding Author

*Tel.: +44 1483 682762. Fax: +44 1483 682135. E-mail: P.Kumar@surrey.ac.uk, Prashant.Kumar@cantab.net.

Notes

The authors declare no competing financial interest.

■ ACKNOWLEDGMENTS

This work is carried out as a part of U.K.−China EPSRC grant (EP/I010912/1), titled as "Multi-scale evaluation of advanced technologies for capturing the CO_2: Chemical looping applied to solid fuels". The authors also thank the Department of Civil and Environmental Engineering at the University of Surrey for additional funding support.

■ REFERENCES

(1) Holloway, S.; Pearce, J. M.; Hards, V. L.; Ohsumi, T.; Gale, J. Natural emissions of CO_2 from the geosphere and their bearing on the geological storage of carbon dioxide. *Energy* **2007**, *32* (7), 1194−1201.

(2) Taseska, V.; Markovska, N.; Causevski, A.; Bosevski, T.; Pop-Jordanov, J. Greenhouse gases (GHG) emissions reduction in a power system predominantly based on lignite. *Energy* **2011**, *36* (4), 2266−2270.

(3) *International Energy Outlook*; Energy Information Administration (EIA): Washington DC, 2008. http://www.eia.gov/forecasts/ieo/more_highlights.cfm (accessed Feb. 12, 2013)

(4) Cayan, D. R.; Maurer, E. P.; Dettinger, M. D.; Tyree, M.; Hayhoe, K. *Climate Change Scenarios for the California Region*; Springer Science: New York, 2008.

(5) Longwell, J. P.; Rubin, E. S.; Wilson, J. Coal: Energy for the future. *Prog. Energy Combust. Sci.* **1995**, *21* (4), 269−360.

(6) Minchener, A. J.; McMullan, J. T. Sustainable clean coal power generation within a European context—The view in 2006. *Fuel* **2007**, *86* (14), 2124−2133.

(7) Boot-Handford, M. E.; Abanades, J. C.; Anthony, E. J.; Blunt, M. J.; Brandani, S.; Mac Dowell, N.; Fernandez, J. R.; Ferrari, M.-C.; Gross, R.; Hallett, J. P.; Haszeldine, R. S.; Heptonstall, P.; Lyngfelt, A.; Makuch, Z.; Mangano, E.; Porter, R. T. J.; Pourkashanian, M.; Rochelle, G. T.; Shah, N.; Yao, J. G.; Fennell, P. S. Carbon capture and storage update. *Energy Environ. Sci.* **2014**, *7*, 130−189.

(8) Chiesa, P.; Consonni, S.; Kreutz, T.; Robert, W. Co-production of hydrogen, electricity and CO_2 from coal with commercially ready technology. Part A: Performance and emissions. *Int. J. Hydrogen Energy* **2005**, *30* (7), 747−767.

(9) Damen, K.; Troost, M. v.; Faaij, A.; Turkenburg, W. A comparison of electricity and hydrogen production systems with CO_2 capture and storage. Part A: Review and selection of promising conversion and capture technologies. *Prog. Energy Combust. Sci.* **2006**, *32* (2), 215−246.

(10) Cormos, C.-C. Assessment of hydrogen and electricity co-production schemes based on gasification process with carbon capture and storage. *Int. J. Hydrogen Energy* **2009**, *34* (15), 6065−6077.

(11) Cormos, C.-C. Evaluation of energy integration aspects for IGCC-based hydrogen and electricity co-production with carbon capture and storage. *Int. J. Hydrogen Energy* **2010**, *35* (14), 7485−7497.

(12) Cormos, C.-C. Evaluation of syngas-based chemical looping applications for hydrogen and power co-generation with CCS. *Int. J. Hydrogen Energy* **2012**, *37* (18), 13371−13386.

(13) Li, F.; Fan, L.-S. Clean coal conversion processes—Progress and challenges. *Energy Environ. Sci.* **2008**, *1* (2), 248−267.

(14) Kunze, C.; Riedl, K.; Spliethoff, H. Structured exergy analysis of an integrated gasification combined cycle (IGCC) plant with carbon capture. *Energy* **2011**, *36* (3), 1480−1487.

(15) Wang, H.; Xu, Li.; Kim, H. *Exergy Analysis of CO_2 Capture from Syngas at Pre-combustion in IGCC Power Plant*; Ajou University: Korea, 2007; Vol. *11*, pp 109−112.

(16) Anheden, M.; Svedberg, G. Exergy analysis of chemical-looping combustion systems. *Energy Convers. Manage.* **1998**, *39* (16−18), 1967−1980.

(17) Brunetti, A.; Drioli, E.; Barbieri, G. Medium/high temperature water gas shift reaction in a Pd-Ag membrane reactor: An experimental investigation. *RSC Adv.* **2012**, *2* (1), 226−233.

(18) Li, Y.; Fu, Q.; Flytzani-Stephanopoulos, M. Low-temperature water−gas shift reaction over Cu- and Ni-loaded cerium oxide catalysts. *Appl. Catal. B: Environ.* **2000**, *27* (3), 179−191.

(19) Bracht, M.; Alderliesten, P. T.; Kloster, R.; Pruschek, R.; Haupt, G.; Xue, E.; Ross, J. R. H.; Koukou, M. K.; Papayannakos, N. Water−

gas shift membrane reactor for CO_2 control in IGCC systems: Techno-economic feasibility study. *Energy Convers. Manage.* **1997**, *38* (Supplement,(0)), S159−S164.
(20) Kohl, A. L.; Nielsen, R. B. Chapter 8 Sulfur Recovery Processes. In *Gas Purification (Fifth ed.)*; Gulf Professional Publishing: Houston, 1997; pp 670−730.
(21) Casas, N.; Schell, J.; Joss, L.; Mazzotti, M. A parametric study of a PSA process for pre-combustion CO_2 capture. *Sep. Purif. Technol.* **2013**, *104* (0), 183−192.
(22) Schell, J.; Casas, N.; Marx, D.; Mazzotti, M. Precombustion CO_2 capture by pressure swing adsorption (PSA): Comparison of laboratory PSA experiments and simulations. *Ind. Eng. Chem. Res.* **2013**, *52* (24), 8311−8322.
(23) Fan, L.-S.; Zeng, L.; Wang, W.; Luo, S. Chemical looping processes for CO_2 capture and carbonaceous fuel conversion—Prospect and opportunity. *Energy Environ. Sci.* **2012**, *5* (6), 7254−7280.
(24) Li, F.; Zeng, L.; Velazquez-Vargas, L. G.; Yoscovits, Z.; Fan, L.-S. Syngas chemical looping gasification process: Bench-scale studies and reactor simulations. *AIChE J.* **2010**, *56* (8), 2186−2199.
(25) Cleeton, J. P. E.; Bohn, C. D.; Müller, C. R.; Dennis, J. S.; Scott, S. A. Clean hydrogen production and electricity from coal via chemical looping: Identifying a suitable operating regime. *Int. J. Hydrogen Energy* **2009**, *34* (1), 1−12.
(26) Erlach, B.; Schmidt, M.; Tsatsaronis, G. Comparison of carbon capture IGCC with pre-combustion decarbonisation and with chemical-looping combustion. *Energy* **2011**, *36* (6), 3804−3815.
(27) Zeng, L.; He, F.; Li, F.; Fan, L.-S. Coal-direct chemical looping gasification for hydrogen production: Reactor modeling and process simulation. *Energy Fuels* **2012**, *26* (6), 3680−3690.
(28) *Aspen Plus IGCC Model*; 2008.
(29) Dincer, I.; Rosen, A. *Exergy: Energy, Environment, and Sustainable Development*; Elsvier: Oxford, U.K., 2007.
(30) Szargut, J.; Morris, D. R.; Stewart, F. R. *Exergy Analysis of Thermal, Chemical, and Metallurgical Processes*; Springer-Verlag GmbH & Co. K: Berlin and Heidelberg, 1988.
(31) El-Emam, R. S.; Dincer, I.; Naterer, G. F. Energy and exergy analyses of an integrated SOFC and coal gasification system. *Int. J. Hydrogen Energy* **2012**, *37* (2), 1689−1697.
(32) Cormos, C.-C. Evaluation of iron based chemical looping for hydrogen and electricity co-production by gasification process with carbon capture and storage. *Int. J. Hydrogen Energy* **2010**, *35* (6), 2278−2289.
(33) *IEA Report: Cost and Performance of Carbon Dioxide Capture from Power Generation*; International Energy Agency (IEA): Paris, 2011. (accessed July 22, 2013)
(34) Liszka, M.; Tuka, J. Parametric study of GT and ASU integration in case of IGCC with CO_2 removal. *Energy* **2012**, *45* (1), 151−159.
(35) Wheeler, F. *Decarbonization of Fossil Fuels*; IEA: Paris, 1996. (accessed July 30, 2013)
(36) Doctor, M. J.; Chess, K. L,; Brockmeier, N. F. *Hydrogen Production and CO_2 Recovery, Transport and Use from a KRW Oxygen-Blown Gasification Combined-Cycle System*; Argonne National Laboratory: Argonne, 1999.
(37) Klett, M. G.; White, J. S.; Schoff, R. L.; Buchanan, T. L. Plant performance and cost comparisons. In *Hydrogen Production Facilities*; National Energy Technology Laboratory: Reading, PA, 2002.
(38) Parsons, E. L. *Advanced Fossil Power Systems Comparison Study*; National Energy Technology Laboratory: Pittsburgh, PA, 2002.
(39) Chiesa, P.; Lozza, G.; Malandrino, A.; Romano, M.; Piccolo, V. Three-reactors chemical looping process for hydrogen production. *Int. J. Hydrogen Energy* **2008**, *33* (9), 2233−2245.
(40) Rezvani, S.; Huang, Y.; McIlveen-Wright, D.; Hewitt, N.; Mondol, J. D. Comparative assessment of coal fired IGCC systems with CO_2 capture using physical absorption, membrane reactors, and chemical looping. *Fuel* **2009**, *88* (12), 2463−2472.
(41) Fan, L. S. *Chemical Looping Systems for Fossil Energy Conversions*; John Wiley and Sons, Inc.: Hoboken, NJ, 2010.
(42) Liu, Y.; Li, Z.-s.; Xu, L.; Cai, N. Effect of sorbent type on the sorption enhanced water−gas shift process in a fluidized bed reactor. *Ind. Eng. Chem. Res.* **2012**, *51* (37), 11989−11997.
(43) Fan, L. S.; Li, F. Chemical looping technology and its fossil energy conversion applications. *Ind. Eng. Chem. Res.* **2010**, *49*, 10200−10211.